8-12-1991

Breakdown of a Wire-to-Plane Discharge: Transient Effects

Milind A. Jog
University of Pennsylvania

Ira M. Cohen
University of Pennsylvania

Portonovo S. Ayyaswamy
University of Pennsylvania, ayya@seas.upenn.edu

Breakdown of a Wire-to-Plane Discharge: Transient Effects

Abstract
A wire-to-plane discharge during the early phases of breakdown has been studied. The discharge has been modeled in a prolate spheroidal coordinate system with the wire shape taken as a hyperboloid of revolution. Four simultaneous coupled, time-dependent, nonlinear partial differential equations describe the electrical discharge. These are the conservation equations for ion and electron densities, the energy equation for electron temperature, and Poisson's equation for the self-consistent electric field. By solving this formulation subject to appropriate initial and boundary conditions, charged particle densities and temperature variations have been obtained as the ionization progresses in the discharge. The results show that both the electron temperature and the charged particle densities increase with the progress of ionization. The effect of different wire polarities is also examined. With a positive wire polarity, the increases in electron temperature and charged particle densities are confined to regions of the discharge in the vicinity of the wire tip. With a negative wire polarity, the breakdown occurs in the entire gap at a faster rate than with a positive wire polarity. The wire polarity affects the magnitude of energy transfer between the particles.

Disciplines
Engineering | Mechanical Engineering

Comments
Suggested Citation:
Jog, Milind A., Ira M. Cohen and Portonovo S. Ayyaswamy. (1991). *Breakdown of a wire-to-plane discharge: Transient effects.* Physics of Plasmas. Vol. 3(12).

Breakdown of a wire-to-plane discharge: Transient effects

M. A. Jog, I. M. Cohen, and P. S. Ayyaswamy
Department of Mechanical Engineering and Applied Mechanics, University of Pennsylvania, Philadelphia, Pennsylvania 19104-6315

(Received 8 May 1991; accepted 12 August 1991)

A wire-to-plane discharge during the early phases of breakdown has been studied. The discharge has been modeled in a prolate spheroidal coordinate system with the wire shape taken as a hyperboloid of revolution. Four simultaneous coupled, time-dependent, nonlinear partial differential equations describe the electrical discharge. These are the conservation equations for ion and electron densities, the energy equation for electron temperature, and Poisson's equation for the self-consistent electric field. By solving this formulation subject to appropriate initial and boundary conditions, charged particle densities and temperature variations have been obtained as the ionization progresses in the discharge. The results show that both the electron temperature and the charged particle densities increase with the progress of ionization. The effect of different wire polarities is also examined. With a positive wire polarity, the increases in electron temperature and charged particle densities are confined to regions of the discharge in the vicinity of the wire tip. With a negative wire polarity, the breakdown occurs in the entire gap at a faster rate than with a positive wire polarity. The wire polarity affects the magnitude of energy transfer between the particles.

I. INTRODUCTION

A fully two-dimensional analysis of the transient electrical breakdown of a wire-to-plane discharge has been described. There have been several studies and reviews on electrical breakdown in parallel plane and nonuniform geometries (see, for example, Refs. 1–5). Most of the analytical studies consider a one-dimensional model and the nonuniformities are taken into account via the initial potential distribution. Two-dimensional analyses of electrical breakdown in a parallel plane geometry have also been carried out.[6,7] Recently, Ramakrishna *et al.*[8] reported a two-dimensional analysis of breakdown of a wire-to-plane discharge; however, the discharge in their study has been considered to be isothermal. Here, we consider a more general formulation. The electron energy gain from the electric field and loss by inelastic collisions are included. The discharge is described by conservation equations for charged particle densities and electron energy together with the Poisson's equation for the self-consistent electric field. The charged particle densities and temperature variations have been obtained for positive as well as negative wire polarities. At a given location, the increase in electron temperature precedes the rapid increase in electron density and the electron temperature decreases as the ionization progresses. With a negative wire polarity, the breakdown occurs in the entire gap at a faster rate than with a positive wire polarity. Discharges such as the one studied here, are used, for example, in the melting of wires in the ball-bonding process of semiconductor chips.[9]

In the ball-bonding process, a fine metal wire (typically 25 μm diameter) is heated from below by an electric discharge across an air gap. (Sometimes an inert or reducing gas is used at atmospheric pressure.) After the initial breakdown, treated in this paper, a steady discharge of brief duration heats and melts the wire. Surface tension causes the molten metal to roll up and form a ball. The discharge is then terminated, the ball solidifies, and is pressed down by a bonding machine onto a pad on a semiconductor chip to form a (ball) bond. Wire is looped over to the mounting (lead) frame where a second bond is made to connect the chip circuitry to the outside.

II. MATHEMATICAL FORMULATION

A collision-dominated plasma is adequately described by the continuum conservation equations. Here we consider a collision-dominated, low-energy, two-temperature plasma consisting of three species—electrons, positive ions, and neutrals. We assume that each specie is in equilibrium with its like particle, and the background gas is homogeneous and at rest. Since good collision coupling exists between the heavy particles, ion and neutral particle temperatures are taken to be the same and prescribed as constant. The breakdown is assumed to be axially symmetric. The governing conservation equations are derived in Refs. 10 and 11. These are

$$\frac{\partial N_{e,i}}{\partial t} + \nabla\cdot\Gamma_{e,i} = P(N_e) - R(N_e), \tag{1}$$

where the electron and the ion fluxes are given by

$$\begin{aligned} &\Gamma_{e,i} = -(\mu_{e,i}/e)(\nabla p_{e,i} \pm eN_{e,i}\mathbf{E}), \\ &p_{e,i} = N_{e,i}kT_{e,i}. \end{aligned} \tag{2}$$

The electron temperature is obtained from the energy conservation equation for electrons,

$$\frac{\partial}{\partial t}\left(\frac{3}{2}N_e kT_e\right) + \nabla\cdot\mathbf{q}_e = -e\Gamma_e\cdot\mathbf{E} - Q_{ei}, \tag{3}$$

where

$$\mathbf{q}_e = \tfrac{5}{2}kT_e\Gamma_e - k_e\nabla T_e. \tag{4}$$

The self-consistent electric field is given by Poisson's equation

$$\nabla\cdot\mathbf{E} = (e/\epsilon_0)(N_i - N_e). \tag{5}$$

 0899-8221/91/123532-05$02.00

Here, N represents charged particle number density, T is the temperature, p represents pressure, μ the mobilities, V is the electric potential, $\mathbf{E}$ is the electric field, Q_{ei} is the rate of transfer of energy during inelastic collisions, k is Boltzmann's constant, k_e is the electron thermal conductivity, ϵ_0 is the permittivity of free space, and e is the magnitude of electric charge on an electron. The subscripts e and i are used for electrons and ions, respectively.

At atmospheric pressure, the mean-free path for collisions is about 0.1 μm. The gradient length in this problem is about 10 μm (as can be seen from our results below). Thus a typical length scale for charged particle variation is about 100 mean-free paths, validating a continuum or diffusion model. Even during the subsequent steady discharge, when the ionization may be substantial and the Debye length in the body of the plasma may be as short as the mean-free path, the sheaths adjacent to the electrodes are measured in terms of the *local* Debye length. This is much larger because of the depressed densities in the sheaths due to the absorbing boundary condition. Thus, even the sheaths obey a continuum description.

In the above, $P(N_e) - R(N_e)$ is the net ionization produced by electron impact ionization, thermal ionization, and three-body recombination. Impact ionization is given by

$$P(N_e) = \alpha_i \mu_e E N_e.$$

The primary ionization coefficient α_i is a function of the ratio of electric field to the gas pressure E/p.

$$\alpha_i = A_i p \exp[-B_i/(E/p)].$$

The constants A_i and B_i depend upon the type of gas.[12,13] The Saha equation gives the net thermal ionization and recombination as[14]

$$P(N_e) - R(N_e) = \gamma N_e \left[\frac{2g_i N_n}{g_n} \left(\frac{2\pi m_e k T_e}{h^2} \right)^{3/2} \times \exp\left(-\frac{eV_i}{kT_e} \right) - N_e N_i \right],$$

and the recombination coefficient strongly depends on the electron temperature as [15]

$$\gamma = 1.09 \times 10^{-20} T_e^{-9/2} \ (\mathrm{m^6/sec}).$$

Here the g's are statistical weights, V_i is the ionization potential, and h is Planck's constant.

To calculate the energy transfer during inelastic collisions (Q_{ei}) we consider that successive excitation collisions result in ionization. We assume that each ionization consists of two inelastic collisions and that half of the ionization energy is transferred during each collision.

The discharge is modeled in a prolate spheroidal coordinate system which provides a fine computational grid near the wire tip (see Fig. 1). The wire shape is taken as a hyperboloid of revolution. The prolate spheroidal coordinates are related to the Cartesian coordinates by

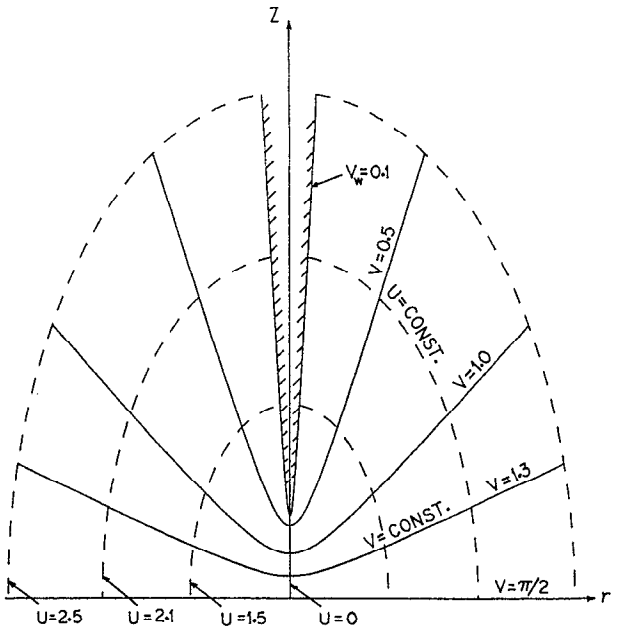

FIG. 1. Schematic of discharge problem showing prolate spheroidal coordinates.

$$x = a \sinh u \sin v \cos \phi,$$
$$y = a \sinh u \sin v \sin \phi, \tag{6}$$
$$z = a \cosh u \cos v.$$

Here a is the semifocal distance used as a normalization length. We define a "wire diameter" d as twice the tip radius of curvature. Thus $d = 2L \tan^2 v_w$, $L = a \cos v_w$, where L is the interelectrode gap.

The coordinates shown are natural for this problem, as both electrodes could be taken as coordinate surfaces. Moreover the initial condition for the electrostatic potential has a simple form and boundary conditions are easily stated. The complexity of the metric coefficients is of no consequence in our numerical solution.

We introduce the following normalizations to obtain a nondimensional formulation. The temperatures are normalized by the ambient temperature T_∞. The number densities are normalized by the number density value which results in a Debye length equal to the wire diameter $N_R = kT_\infty \epsilon_0/(e^2 d^2)$. The potential and the electric field are normalized by $V_R = kT_\infty/e$ and $E_R = V_R/d$, respectively.

With this normalization the governing equations, the boundary conditions, and the initial conditions are

$$\frac{\partial n_{e,i}}{\partial t} + \frac{F_{e,i}}{(\sinh^2 u + \sin^2 v)} \frac{1}{\sinh u} \frac{\partial}{\partial u} \left[\sinh u \left(\frac{\partial (T_{e,i} n_{e,i})}{\partial u} \pm n_{e,i} \frac{\partial \psi}{\partial u} \right) \right] + \frac{F_{e,i}}{(\sinh^2 u + \sin^2 v)} \frac{1}{\sin v} \frac{\partial}{\partial v} \times \left[\sin v \left(\frac{\partial (T_{e,i} n_{e,i})}{\partial v} \pm n_{e,i} \frac{\partial \psi}{\partial v} \right) \right] = \exp\left(-\frac{B_i}{E} \right) n_e E + C_1 C_2 n_e T_e^{-3} \exp\left(-\frac{\psi_i}{T_e} \right) - C_1 T_e^{-9/2} n_e^2 n_i, \tag{7}$$

$$\frac{\partial}{\partial t}(n_e T_e)+\frac{5}{3}\frac{F_e}{(\sinh^2 u+\sin^2 v)}\frac{1}{\sinh u}\frac{\partial}{\partial u}\left[\sinh u T_e\left(\frac{\partial}{\partial u}(T_e n_e)-n_e\frac{\partial\psi}{\partial u}\right)\right]$$
$$+\frac{5}{3}\frac{F_e}{(\sinh^2 u+\sin^2 v)}\frac{1}{\sin v}\frac{\partial}{\partial v}\left[\sin v T_e\left(\frac{\partial}{\partial v}(T_e n_e)-n_e\frac{\partial\psi}{\partial v}\right)\right]$$
$$+\frac{2}{3}\frac{F_c}{(\sinh^2 u+\sin^2 v)}\left[\frac{1}{\sinh u}\frac{\partial}{\partial u}\left(\sinh u\frac{\partial T_e}{\partial u}\right)+\frac{1}{\sin v}\frac{\partial}{\partial v}\left(\sin v\frac{\partial T_e}{\partial v}\right)\right]$$
$$=\frac{2}{3}\frac{F_e}{(\sinh^2 u+\sin^2 v)}\left(\frac{\partial n_e T_e}{\partial u}\frac{\partial\psi}{\partial u}+\frac{\partial n_e T_e}{\partial v}\frac{\partial\psi}{\partial v}\right)$$
$$+\frac{2}{3}\frac{F_e n_e}{(\sinh^2 u+\sin^2 v)}\left[\left(\frac{\partial\psi}{\partial u}\right)^2+\left(\frac{\partial\psi}{\partial v}\right)^2\right]-Q_{ei}, \tag{8}$$

$$\frac{1}{(\sinh^2 u+\sin^2 v)}\left[\frac{1}{\sinh u}\frac{\partial}{\partial u}\left(\sinh u\frac{\partial\psi}{\partial u}\right)+\frac{1}{\sin v}\frac{\partial}{\partial v}\left(\sin v\frac{\partial\psi}{\partial v}\right)\right]=\frac{a^2}{d^2}(n_e-n_i), \tag{9}$$

where

$$F_{e,i}=\frac{\mu_{e,i}V_R t_R}{a^2},\quad F_c=\frac{k_e t_R}{(N_R a^2 k)},\quad t_R=\frac{1}{(A_i p\mu_e E_R)},$$

$$C_1=1.09\times10^{-20}N_R^2 T_\infty^{-9/2}t_R,$$

$$C_2=4.8186\times10^{21}N_n g_i T_\infty^{3/2}/(g_n N_R^2).$$

The boundary conditions are

on the wire electrode:

$$v=v_w,\quad \psi=\psi_w,\quad n_{e,i}=n_0,\quad \text{and}\quad T_e=T_w;$$

on the planar electrode:

$$v=\pi/2,\quad \psi=0,\quad n_{e,i}=n_0,\quad \text{and}\quad T_e=T_w;$$

on the axis:

$$u=0,\quad \frac{\partial}{\partial u}=0;$$

and

away from the axis:

$$u\to\infty,\quad \frac{\partial\psi}{\partial u}\to0,\quad n_{e,i}\to n_0,\quad \text{and}\quad T_e\to T_\infty.$$

The electrodes are considered to be nearly perfect absorbing surfaces. The number density n_0 is the small ambient density due to the omnipresent background radiation. This is assigned to the electrodes to avoid singular behavior which may result from requiring zero density at the electrodes. This also accounts for the weak reflection and emission from the electrode surfaces.

Initial conditions: The initial charged particle densities are taken to be n_0 and the initial temperature is T_∞. As the initial charged particle densities are very small, the initial electric field is given by the solution to Laplace's equation, $\psi=\psi_w \ln[\tan(v/2)]/\ln[\tan(v_w/2)]$. The initial conditions are

at $t=0$,

$$n=n_0,\quad T=T_\infty,\quad \text{and}\quad \psi=\frac{\psi_w\ln[\tan(v/2)]}{\ln[\tan(v_w/2)]}.$$

III. RESULTS AND DISCUSSION

Equations (7)–(9) are the governing equations with the boundary conditions and initial conditions. These equations were solved numerically using the alternating direction implicit method. The diffusion terms were discretized by central differences whereas the drift terms were discretized by upwind differences. Initially when the charged particle number densities are very low, the electron transport due to diffusion is very small compared to the transport due to electron drift. As the number densities increase, the drift and the diffusion effects become comparable in the u direction whereas in the v direction drift terms remain much larger than the diffusion terms. The program was run on the Pittsburgh Supercomputing Center's CRAY Y/MP and each run took about 1.5 h. The parameters used for the calculations are $d=1\times10^{-5}$ m, $L=5\times10^{-4}$ m, $N_0=6\times10^8$ m^{-3}, $N_n=1.47\times10^{25}$ m^{-3}, $N_R=2.36\times10^{16}$ m^{-3}, $p=1.01\times10^5$ Pa, $T_\infty=500$ K, $T_i=500$ K, $t_R=1.02\times10^{-8}$ sec, $A_i=6.5$ m/N, $B_i=191.21$ m/N, $\mu_e=0.0348$ m^2/V sec. The medium is air. These parameters are typical of the ball formation process for ball bonding of semiconductor chips. Results are obtained for an applied voltage of 2500 V for negative as well as positive wire polarity.

We first discuss results for a positive wire.

A. Positive wire polarity

Figure 2 shows the variations of charged particle densities at several locations on the discharge axis. The electron densities rise and then become constant when a balance is achieved between net production and drift. This rise in number density is different for different locations. The electric field decreases from the wire to the plane which results in a corresponding decrease in production of charged particles. Since electrons move toward the wire, both the effects lead to successively higher number densities toward the wire. It can be seen that the breakdown has not reached much beyond $Z=0.8$. The electrons gain energy from the electric field as they drift toward the anode wire. This confines the electron temperature increase to regions of the discharge in the vicinity of the wire tip. This can be seen from Fig. 3. The temperature increases as the ionization proceeds. In this case the ionization levels are lower than those with negative wire polarity, less energy is lost by the electrons, and the drop in electron temperature is consequently lower. Figure 4 shows

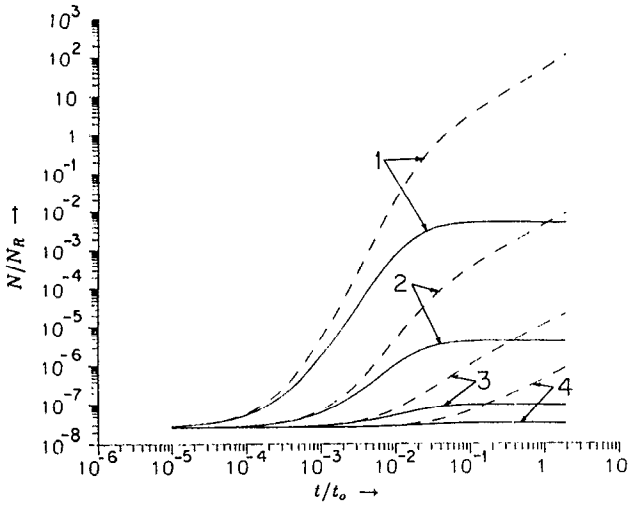

FIG. 2. Variation of charged particle densities with time at various locations on the discharge axis, $p = 1$ atm in air, $V_w = 2500$ V. Legend: (1) $Z = 0.99$, (2) $Z = 0.95$, (3) $Z = 0.9$, (4) $Z = 0.8$; $Z = z/L$. Solid lines: electron number density; dashed lines: ion number density.

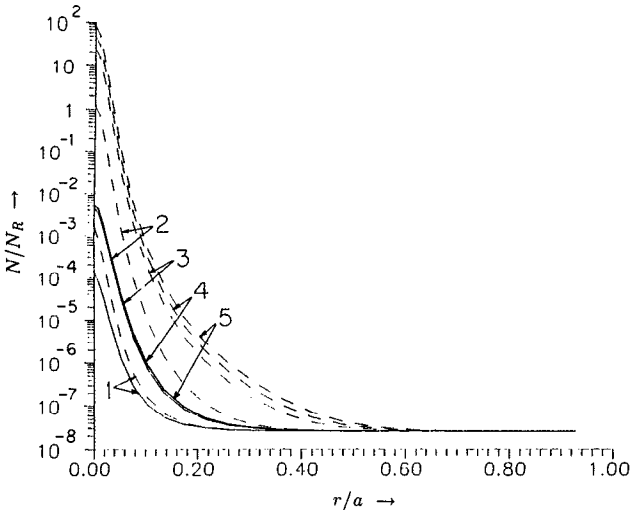

FIG. 4. Radial distribution of charged particle densities, $p = 1$ atm in air, $V_w = 2500$ V. Legend: (1) $t = 5\times10^{-3}$, (2) $t = 5\times10^{-2}$, (3) $t = 0.5$, (4) $t = 1$, (5) $t = 1.5$. Solid lines: electron number density; dashed lines: ion number density.

the radial variations of charged particle densities. As the electrons move toward the wire electrode, the inward electric field causes a drift toward the discharge axis. This confines the higher electron densities to within a few wire diameters of the discharge axis. The corresponding electron temperature variations are shown in Fig. 5.

B. Negative wire polarity

Figure 6 shows the variations of charged particle densities at various locations along the discharge axis. The production of charged particles begins near the wire tip. As the electron number density increases, electrons move toward the planar electrode resulting in increased number densities of charged particles due to increased ionization and drift. This rise in number density occurs at progressively later times for locations farther from the wire tip. Comparing this with the variation of charged particle densities along the discharge axis for positive wire polarity (Fig. 2) we see that the charged particle densities are higher in the vicinity of the wire tip for positive wire polarity. With the negative wire polarity, charged particle densities increase toward the planar electrode. As the ion drift is small and the ionization rate is proportional to the electron number densities, large ion number densities occur at the locations where the electron densities are large. The temperature variations for the same locations considered in Fig. 6 are shown in Fig. 7. As

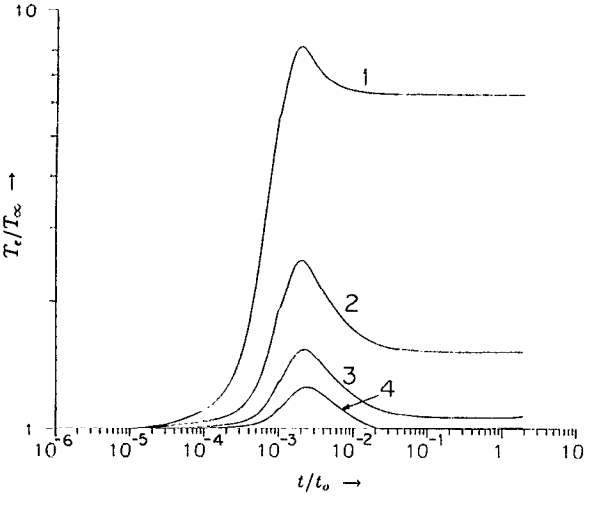

FIG. 3. Variation of electron temperature with time at various locations on the discharge axis, $p = 1$ atm in air, $V_w = 2500$ V. Legend: (1) $Z = 0.99$, (2) $Z = 0.95$, (3) $Z = 0.9$, (4) $Z = 0.8$.

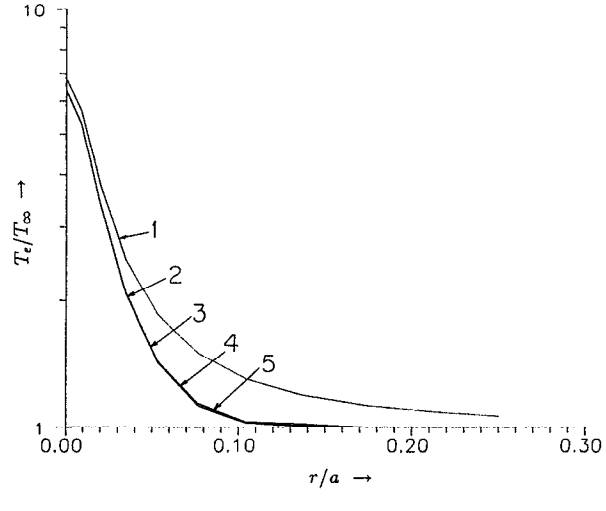

FIG. 5. Radial electron temperature distribution, $p = 1$ atm in air, $V_w = 2500$ V. Legend: (1) $t = 5\times10^{-3}$, (2) $t = 5\times10^{-2}$, (3) $t = 0.5$, (4) $t = 1$, (5) $t = 1.5$.

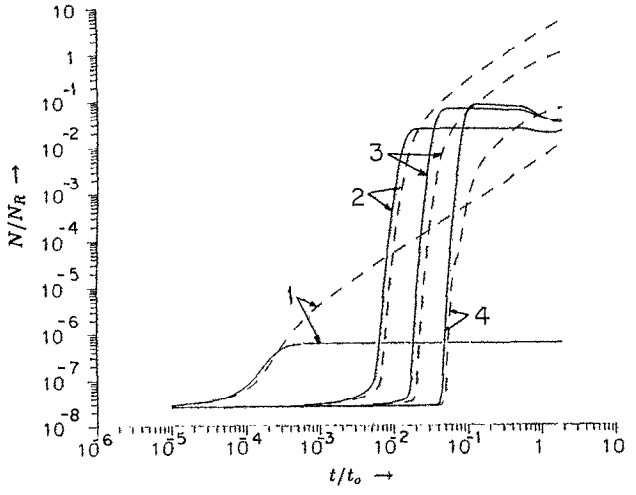

FIG. 6. Variation of charged particle densities with time at various locations on the discharge axis, $p = 1$ atm in air, $V_w = -2500$ V. Legend: (1) $Z = 0.99$, (2) $Z = 0.9$, (3) $Z = 0.8$, (4) $Z = 0.67$. Solid lines: electron number density; dashed lines: ion number density.

the ionization progresses outward from the wire tip, the charged particle densities increase very rapidly. This rapid increase in number density is preceded by an increase in electron temperature at a given location. Electrons gain energy from the electric field and the electron temperature increases. This can be seen from the rising part of the temperature curve in Fig. 7. These electrons lose their energy in inelastic collisions with the neutrals. As the ionization rate increases, electrons lose progressively more energy in the ionization process, which results in a decrease in electron temperature. Later, a balance is achieved between gain and loss of electron energy resulting in a constant electron temperature. In this circumstance, electron densities on the axis are almost constant as the ionization rate on the discharge

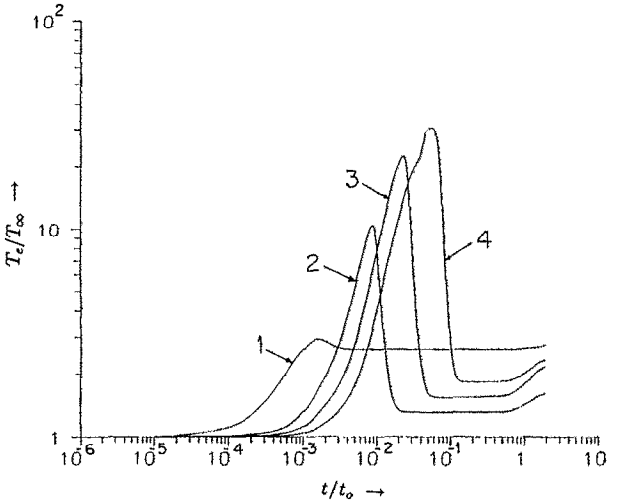

FIG. 7. Variation of electron temperature with time at various locations on the discharge axis, $p = 1$ atm in air, $V_w = -2500$ V. Legend: (1) $Z = 0.99$, (2) $Z = 0.9$, (3) $Z = 0.8$, (4) $Z = 0.67$.

axis essentially compensates for the electron drift. The ion mobility is much smaller than that of the electrons resulting in a small ion drift, and ion densities continue to rise. After this plateau, the electron temperature starts increasing again. This may lead to the second phase of breakdown where thermal ionization will become increasingly important and charged particle densities will grow still larger to complete the process of breakdown.

IV. CONCLUSIONS

We have studied electrical breakdown of a wire-to-plane discharge at atmospheric pressure. The discharge is described by conservation equations for charged particle densities and electron energy together with Poisson's equation for the self-consistent electric field. These governing equations have been numerically integrated to obtain the variations of charged particle densities and electron temperature for negative as well as positive wire polarities. From this study we draw the following conclusions:

(1) The breakdown occurs in the entire gap at a faster rate with negative wire polarity than with positive wire polarity.

(2) With positive wire polarity the maxima in charged particle density and electron temperature occur on the discharge axis, whereas with the negative wire, the maxima in charged particle density and electron temperature occur a few wire diameters away from the discharge axis.

(3) The steep rise in electron temperature precedes the rapid increase in electron density at a given location, but the electron temperature decreases as the ionization continues.

ACKNOWLEDGMENTS

This work was supported by the National Science Foundation under Grants No. DMC 8709537 and No. DDM 9000573. Support for numerical computations was provided by the Pittsburgh Supercomputing Center (PSC) under Grants No. DMC 0000000/8513128 and No. DMC 890001P. Computations were performed on PSC's CRAY Y/MP.

[1]H. Raether, *Electron Avalanches and Breakdown in Gases* (Butterworths, London, 1964).
[2]J. Dutton, in *Electrical Breakdown in Gases*, Wiley Series in Plasma Physics, edited by J. M. Meek and J. D. Craggs (Wiley, New York, 1978), Chap. 3.
[3]E. E. Kunhardt, IEEE Trans. Plasma Sci. **PS-8**, 130 (1980).
[4]R. S. Sigmond, in Ref. 2, Chap. 4.
[5]R. T. Waters, in Ref. 2, Chap. 5.
[6]K. Yoshida and H. Tagashira, J. Phys. D **9**, 435 (1976).
[7]J. P. Novak and R. Bartnikas, J. Appl. Phys. **62**, 3605 (1987).
[8]K. Ramakrishna, I. M. Cohen, and P. S. Ayyaswamy, J. Appl. Phys. **65**, 41 (1989).
[9]L. J. Huang, M. A. Jog, I. M. Cohen, and P. S. Ayyaswamy, Trans. ASME J. Electron. Packag. **113**, 33 (1991).
[10]W. P. Allis, in *Handbuch der Physik* (Springer-Verlag, Berlin, 1956), Vol. XXI, pp. 384–444.
[11]D. R. Wilkins and E. P. Gyftopolous, J. Appl. Phys. **37**, 3533 (1966).
[12]S. C. Brown, *Basic Data of Plasma Physics*, 2nd ed. (MIT Press, Cambridge, MA, 1967), p. 182.
[13]A. von Engel, *Ionized Gases*, 2nd ed. (Oxford U.P., London, 1965), p. 180.
[14]M. Mitchner and C. H. Kruger, *Partially Ionized Gases* (Wiley, New York, 1973), p. 78.
[15]E. Hinnov and J. G. Hirshberg, Phys. Rev. **125**, 795 (1962).